

Microscale mode-selective photonic lantern multiplexer compatible with 3D nanoprinting technology

Yoav Dana and Dan M. Marom

Department of Applied Physics, The Hebrew University of Jerusalem, Jerusalem, Israel
Yoav.dana@mail.huji.ac.il

Abstract: We design mode-selective photonic lantern multiplexer using 3D waveguides made of photopolymer core and air cladding. Although the waveguides exhibit high index contrast, low loss (0.14dB), MDL (-0.06db), and mode group crosstalk (-21.2dB) are obtained. © 2022 The Author(s)

1. Introduction

Photonic lanterns consist of an adiabatic spatial transition from a multi-mode optical waveguide to a discrete set of single-mode waveguides, with matching mode and waveguide counts [1]. They can losslessly convert from the multi-mode domain to the single-mode array domain and are an enabling technology for space division multiplexing [2]. Photonic lanterns can be made by fibers that coalesce to one [3], by waveguide inscription in glass using direct laser writing [4], and in photonic integrated circuits [5]. Due to the adiabatic transition requirement, photonic lantern (PL) devices are typically long and utilize low index contrast waveguides. The ability to 3D print optical waveguides in a photopolymer using direct laser writing [6] results in air-cladded structures having very small transverse dimensions to remain single mode [7]. Symmetric PLs, in which all single-mode fibers are identical, are non-mode selective as there is no one-to-one correspondence between an input source and a specific mode of the MMF [8]. Because degenerate modes in MMFs strongly couple with each other, it is not necessary to make the photonic lantern selective between degenerate modes within the same group [8]. In this work we report the design of a three-mode selective PL compatible with micro-scale 3D optical waveguides, using machine learning method for optimization, exhibiting very low insertion loss, mode-dependent loss and crosstalk between the two mode groups.

2. Device description and design

The PL device we envision can be made of a photopolymer that undergoes polymerization using two-photon absorption of a writing laser beam, providing the ability to fabricate arbitrary three-dimensional sub-micron structures that are difficult—if not impossible—to fabricate using conventional techniques. As the PL is designed to support only three modes in this work, the structure consists of three separate single-mode waveguides on one end and a three-mode waveguide on the other end with an adiabatic transition over 100 μm length disposed in between (Fig. 1-a). Since only the photoexcited areas are polymerized and the remaining photopolymer is cleared away, the waveguides exhibit a high index contrast between core ($n_{core} \cong 1.5$) and cladding (air at $n_{clad} \cong 1$). The single-mode waveguides have circular cross-section (diameter of 1 μm , supporting the fundamental mode HE_{11}) while the triple mode output waveguide is 1.6 μm diameter, with the PL designed for operation at $\lambda_0=1.55 \mu\text{m}$ (vacuum wavelength). In order to design a mode selective PL the input single mode waveguides are arranged in an isosceles triangular (Fig. 1-d), with two of the waveguides at the acute triangle angles having the 1 μm diameter and the waveguide at the right angle corner is of 1.06 μm diameter. The differing diameters are a necessary condition for maintaining mode group separation. Without it, a non-mode preserving photonic lantern is formed [9]. Each HE_{11} spatial mode supports two orthogonal polarizations (see Fig. 1-c), hence the PL is a 6-input, 6-output device. The output modes, designated as

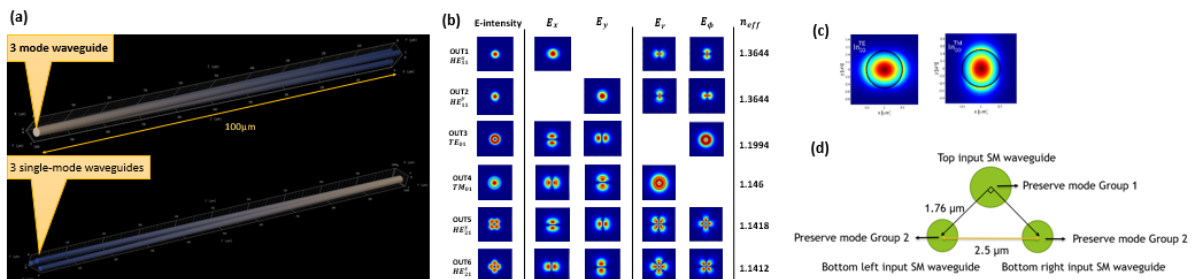


Fig. 1: (a) Visualization of the PL design. (b) The output waveguide supported modes and input modes. (c) input waveguide supported modes. (d) demonstrates the input SM waveguides arrangement.

Out1-Out6 (Fig.1-b), can be subdivided to two mode groups: Group 1 carries the fundamental mode HE_{11} (designated Out1-Out2) and Group 2 contains the TE_{01} , TM_{01} , and HE_{21} modes (designated Out3-Out6). Note that in low index contrast waveguides the Group 2 modes are nearly degenerate, whereas in our case there is larger momentum separation between them (yet still well separated from Group 1). The spatial modes and the propagation through the PL device were all simulated with Ansys Lumerical Device Suite.

3. Optimization process

The optimization method is based on coupling matrix analysis, which in our case is of dimension 6×6 and each matrix element is the complex coupling coefficient between input to output mode combinations. The coupling coefficients are found using an FDTD solver, propagating each single-mode input of either polarization and gauging the modal content at the distal end. From the eigenvalues of the coupling matrix, σ_i , we calculate the insertion loss (IL) and the mode dependent loss (MDL), as defined in Eq (1):

$$IL = \frac{1}{6} \sum_{i=1}^6 |\sigma_i|^2, \quad MDL = \frac{|\sigma_{min}|^2}{|\sigma_{max}|^2} \quad (1)$$

Since the waveguides are defined by 3D printing, we have multiple options for geometrical design of the PL. In the optimization process we defined three parameters for describing the waveguide evolution. First is the waveguides geometrical path from the input (SM) to the output (MM), defined by a power function of variable exponent, n (Fig. 2-a). The second parameter is the waveguides cross-section expansion rate, since the waveguides starts from single-mode and end in multimode, hence the diameter is also changing according to power function throughout the photonic lantern. The third degree of freedom is the diameter of the single-mode waveguide at the triangle's right angle, which breaks the symmetry and enables mode selectivity.

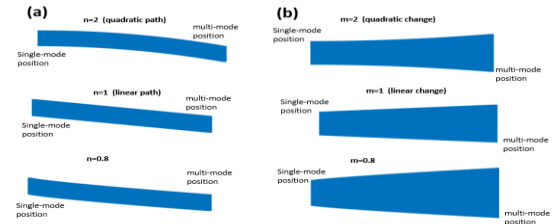


Fig. 2: (a) Waveguide path from the input (single mode side) to the output (multi-mode). controlled by an exponent n . (b) Diameter rate of change from single-mode diameter ($1\mu\text{m}$) to multimode diameter ($1.6\mu\text{m}$), controlled by a single exponent, m .

Our optimization goal is to maintain low insertion loss with low crosstalk between the two mode groups. Due to the long run time of the FDTD simulation and the optimization over three degrees of freedom, we employed a machine learning model known as polynomial fit regression [10]. We collected 200 samples of FDTD simulations, where in each simulation the three parameters were randomly chosen between a range of values of interest, waveguide path and cross-section rate of change in the interval of $[0.8, 2]$ while the waveguide destined to preserve the fundamental mode in the interval of $[1.0, 1.12] \mu\text{m}$. The structure of the data set (Table 1) is divided to a design matrix, X , which contains the randomly chosen optimization parameters, and seven response vectors y_{0-6} which contain 7 different metrics extracted from the coupling matrix for each realization in X . Response vector y_0 contains the insertion loss measured from each simulation, while response vectors y_{1-6} contain the power coupling from each input mode to its destination mode group. To ensure low crosstalk between groups and low insertion losses, the goal is to maximize all seven metric responses. Since there are multiple vectors to predict, we applied for each response vector a different polynomial fitting function to the input degrees of freedom. The polynomial fit for estimating the insertion loss, y_0 , achieved an average training error of $\sim 4 \cdot 10^{-7}$ using polynomial degree of 3, and $\sim 5 \cdot 10^{-5}$ error for the rest of the response vectors, y_{1-6} , using polynomial degree of 4. The training errors are calculated by the MSE metric:

$$MSE = \frac{1}{n} \sum_i^n (y_{estimated}^i - y_{test}^i)^2 \quad (2)$$

Where n in Eq. 2 is the number of samples. After fitting a regression model to the simulation data, we need to seek the optimal design over the full three-dimensional search space. We randomly sample the space using 27000 triplet

Table 1: Data set structure.

Design matrix X			Seven response vectors $y_{(0-6)}$						
x_1	x_2	x_3	y_0	y_1	y_2	y_3	y_4	y_5	y_6
Waveguide path	Cross section rate of change	Top waveguide cross section radius	Insertion loss	Coupling of mode in1 to group1	Coupling of mode in2 to group1	Coupling of mode in3 to group 2	Coupling of mode in4 to group 2	Coupling of mode in5 to group 2	Coupling of mode in6 to group 2

points (evaluated using the polynomial estimator), and using the predicted metric vector y (now trivially computed), we extract the optimal design parameters from the prediction set seeking to concurrently maximize all y_{1-6} .

4. Results

Using the polynomial descriptors, we seek an optimal design by defining the three shape parameters that achieve the best performance metrics. For these input parameters, another FDTD simulation is performed to ascertain the prediction from the fitted polynomial functions. The estimated results and the simulation results are within accuracy of 10^{-3} (comparison shown in Table 2). The IL is 97.6% (-0.14dB) and MDL is 98.5% (-0.06dB). From the power coupling matrix (see Fig. 3-a), we observe a very low crosstalk between the two different mode groups. The worst crosstalk from a single waveguide excitation to the wrong group is 0.0076 (-21.2 dB). To visualize the operation of the mode-selective PL, the intensity profile at the multimode end is displayed when the excitation is from the single mode waveguide that remains in the fundamental group and when the excitation is destined to the second mode group (where the interference of the higher order modes is observed, see Fig. 3-b).

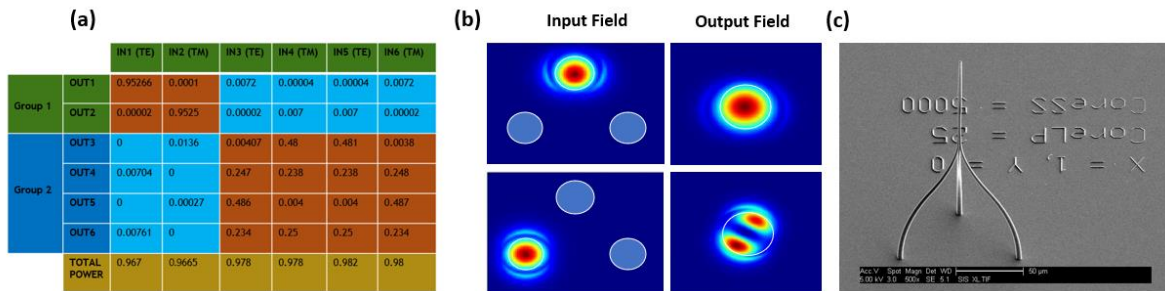


Fig. 3: (a) Optimal power coupling matrix, (b) visualization of modes at excitation and at distal end. (c) initial 3D print of the PL.

Table.2. FDTD simulation compared to regression results.

	y_0	y_1	y_2	y_3	y_4	y_5	y_6
Estimation	0.9759	0.9522	0.9525	0.971	0.973	0.9739	0.9726
simulation	0.976	0.9526	0.9526	0.972	0.974	0.974	0.973

5. Conclusions

We demonstrated the feasibility of shrinking a three-mode selective photonic lantern to multi-micron scale, based on high refractive index waveguides, while retaining low device losses (-0.14dB) and low crosstalk between different mode groups (~-21dB). Due to a large number of degrees of freedom, finding an optimal solution is a major challenge and more methods and algorithms will be examined in the near future, along to upscaling the number of mode groups and 3D printing the PL for assessing its actual performance (Fig. 3-c demonstrates the feasibility of 3D printing PL of this scale).

6. References

- [1] T. A. Birks, et al., "The photonic lantern," *Adv. Opt. Photon.* 7, 107-167 (2015).
- [2] N. K. Fontaine, et al., "Geometric requirements for photonic lanterns in space division multiplexing," *Opt. Express* 20, 27123-27132 (2012).
- [3] S. G. Leon-Saval, et al., "Multimode fiber devices with single-mode performance," *Opt. Lett.* 30, 2545-47 (2005).
- [4] R. R. Thomson, et al., "Ultrafast laser inscription of an integrated photonic lantern," *Opt. Express* 19, 5698-5705 (2011).
- [5] D. Yi, et al., "Integrated Multimode Waveguide With Photonic Lantern for Speckle Spectroscopy," *IEEE J. Quantum Electron.* 57(1), 1-8 (2021).
- [6] M. Schumann, et al., "Hybrid 2D-3D optical devices for integrated optics by direct laser writing," *Light Sci Appl* 3, e175 (2014).
- [7] J. Moughames and X. Porte, "3D printed multimode-splitters for photonic interconnects," *Opt. Express* 10(11), 2952-2961 (2020).
- [8] Bin Huang, et al., "All-fiber mode-group-selective photonic lantern using graded-index multimode fibers," *Opt. Express* 23, 224-234 (2015).
- [9] Y. Dana and D. M. Marom, "Microscale photonic lantern multiplexer compatible with 3D printing technology," in *IEEE Photonics Conference*, 2021.
- [10] G. James, et al., *An Introduction to Statistical Learning*, Springer-Verlag, New York (2013), pp. 87-97.